

WeeCare: Towards Handheld Bladder Fullness Sensing with a Conformable Pad

Zhikai Qin
Carnegie Mellon University
zhikaiq@andrew.cmu.edu

Junyi Zhu
University of Michigan
zhujunyi@umich.edu

Siqi Zhang
Carnegie Mellon University
siqizhang@cmu.edu

Justin Chan
Carnegie Mellon University
justinchan@cmu.edu

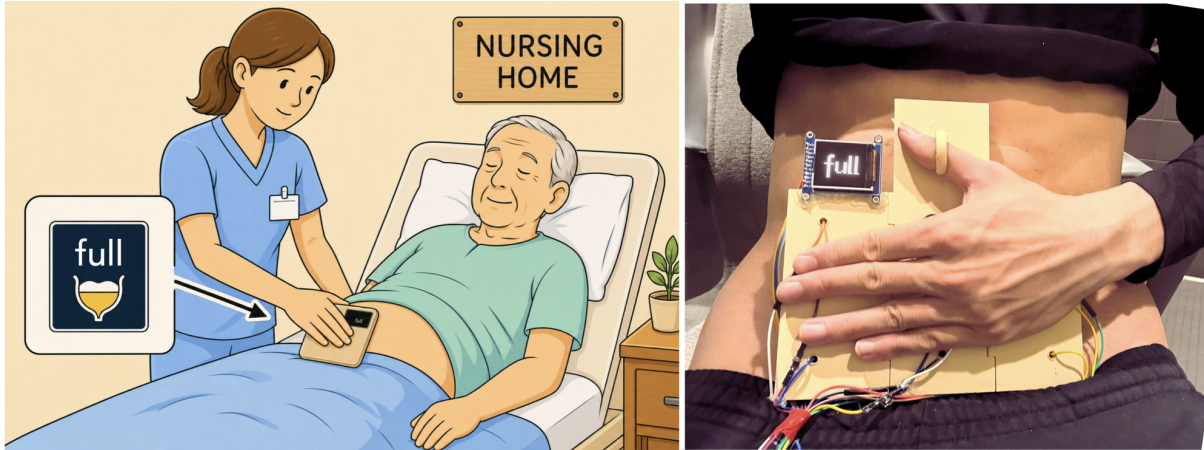


Figure 1: *WeeCare*, a handheld electrical impedance tomography pad for on-demand bladder fullness sensing. (Left) Envisioned use in a care setting for patients with bladder dysfunction who lose the sensation of bladder filling. On-demand bladder fullness sensing has the potential to reduce the need for frequent and unnecessary catheterization. (Right) *WeeCare* prototype, a foldable grid of fabric electrodes that conforms to the abdomen, with an integrated display.

Abstract

Patients with bladder dysfunction often lose the sensation of bladder fullness and cannot void naturally, forcing reliance on fixed-schedule catheterization that is uncomfortable and risks complications. We present *WeeCare*, a handheld conformable pad with fabric electrodes for on-demand bladder fullness sensing using electrical impedance tomography (EIT). The central challenge is that repeated removal and reattachment can introduce variation in electrode position and contact quality. We assess *WeeCare* along three axes: in-silico simulations characterizing electrode layout and noise robustness, in-vitro phantom experiments across urine salinities and filling levels, and an in-vivo human measurement for bladder fullness sensing, voiding, and filling dynamics.

CCS Concepts

• **Human-centered computing** → **Ubiquitous and mobile computing systems and tools.**

Keywords

bladder fullness sensing, electrical impedance tomography

ACM Reference Format:

Zhikai Qin, Siqi Zhang, Junyi Zhu, and Justin Chan. 2026. *WeeCare: Towards Handheld Bladder Fullness Sensing with a Conformable Pad*. In *Proceedings of the 2026 ACM International Joint Conference on Pervasive and Ubiquitous Computing and Proceedings of the 2026 ACM International Symposium on Wearable Computers (UbiComp/ISWC '26)*. ACM, New York, NY, USA, 8 pages. <https://doi.org/XXXXXXXX.XXXXXXX>

1 Introduction

Patients with bladder dysfunction often cannot reliably sense bladder fullness or voluntarily void [8, 37, 43]. This affects individuals with spinal cord injury or spina bifida, where damaged neural pathways impair urinary function [8, 37, 43]. Clean intermittent catheterization is the gold standard for emptying the bladder [8, 19, 43]. However, because patients may have a decreased or absent urge to urinate, catheterization is performed on a fixed schedule, every 2 to 4 hours, rather than when the bladder is actually full [8].

Permission to make digital or hard copies of all or part of this work for personal or classroom use is granted without fee provided that copies are not made or distributed for profit or commercial advantage and that copies bear this notice and the full citation on the first page. Copyrights for components of this work owned by others than the author(s) must be honored. Abstracting with credit is permitted. To copy otherwise, to republish, to post on servers or to redistribute to lists, requires prior specific permission and/or a fee. Request permissions from permissions@acm.org.

UbiComp/ISWC '26, Shanghai, China

© 2026 Copyright held by the owner/author(s). Publication rights licensed to ACM.
ACM ISBN 978-x-xxxx-xxxx-x/YYYY/MM
<https://doi.org/XXXXXXXX.XXXXXXX>

The problem is that catheterizing too early and frequently is uncomfortable, increases caregiver burden, and raises the risks of complications such as urinary tract infections, urethral bleeding, and bladder stones [15, 47]. Conversely, if the bladder overfills before the next scheduled catheterization, it can distend beyond its safe capacity, potentially causing urinary tract damage [26, 43].

Conventionally, ultrasound bladder scanners [18, 41, 42] are used to non-invasively estimate bladder volume but they are typically expensive and bulky with a rigid and uncomfortable probe. Wearable, miniaturized monitors using ultrasound [4, 20, 35], near-infrared spectroscopy [11, 27], or bioelectrical impedance sensing [7, 21, 38], which adhere to the abdomen [40] or integrate into belts [29] and undergarment [49], have been proposed for continuous monitoring, but wearing such systems all day can be uncomfortable.

This gap motivates our research question: *can bladder fullness be sensed non-invasively, comfortably, and on demand?* Such an approach could allow patients to check bladder fullness before deciding whether to catheterize, while also fitting into clinical workflows where caregivers take measurements across multiple patients.

Here, we present *WeeCare*, a handheld conformable pad for on-demand bladder fullness sensing using electrical impedance tomography. Since urine is conductive, changes in bladder volume alter the conductivity of the pelvic region. Electrical impedance tomography (EIT) captures these changes by injecting small electrical currents through surface electrodes and measuring the resulting voltages to reconstruct an internal conductivity map of the bladder [38].

However, the design of a handheld EIT device also introduces a significant challenge which is that repeated removal and application of the device to the skin introduces noise and positional variability [50] that interfere with bladder measurements. We investigate whether bladder fullness can still be obtained through repeated reattachment using a handheld pad along three dimensions.

First, we develop an in-silico simulation to evaluate the robustness of EIT bladder fullness and volume estimation under changes in contact quality and position across different electrode layouts. *Second*, we develop a benchtop phantom model of the bladder and perform in-vitro measurements under repeated removal and reattachment, evaluating volume estimation across urine salinities and bladder filling levels. *Finally*, we perform in-vivo measurements showing we can perform fullness detection under repeated removal and replacement, when the participant moves between measurements, and measure the voiding and filling curve.

2 Background and related work

Bioimpedance and electrical impedance tomography. Bioelectrical impedance sensing measures changes in tissue conductivity when the tissue is exposed to a bio-electrical current with a single global impedance measurement. Given the conductivity of urine, it has been used to estimate bladder filling and volume [7, 9, 39, 49].

Electrical impedance tomography (EIT) extends this by reconstructing spatial conductivity variations from multi-electrode measurements [10, 14, 30, 34]. As shown in Fig. 2a, prior EIT work places electrodes in a ring that encircles the torso, typically embedded in a belt. Current is injected and voltage measured between electrode pairs around this ring, so the sensing field wraps fully around the abdomen and maximizes spatial coverage [34, 38].

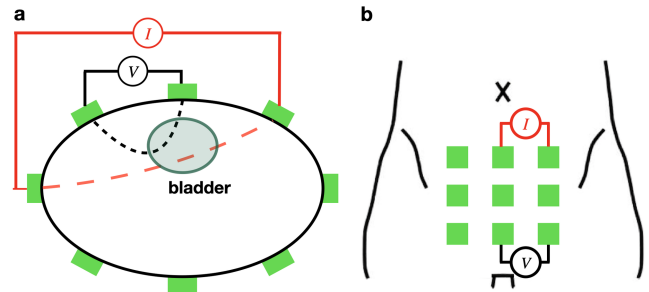


Figure 2: (a) Conventional ring electrode layout in belt form factor. (b) *WeeCare* planar grid electrode layout in handheld pad form factor.

Because the belt stays fixed on the body for an entire filling cycle, these designs can report quantitative bladder volume [7, 38]. However, such a design can be sensitive to patient weight and can be uncomfortable to wear for long periods [3, 7].

In contrast, *WeeCare* uses a planar grid of electrodes in a handheld pad (Fig. 2b). All electrodes sit on a single patch of skin over the bladder rather than encircling the body, so the device can be applied and removed on demand. However, the flexibility of repeated removal and replacement introduces variability in electrode positioning and contact noise between measurements. For our in-vivo testing, we target fullness sensing, a binary empty-versus-full decision, which is sufficient to guide catheterization timing.

Near-infrared spectroscopy. Optical approaches such as near-infrared spectroscopy (NIRS) [2, 12, 27], have been used to estimate urine quantity based on the absorption properties of near-infrared light in human tissue and water using LEDs and photodetectors at the abdomen but are sensitive to tissue variability and have shown limited accuracy in practice.

Ultra-wideband. Ultra-wideband radar has been proposed for contactless measurement of bladder volume [17, 24, 31]. The bladder is illuminated with a UWB pulse and differences in the dielectric properties of urine and the surrounding tissue are detected in the reflections as the bladder fills. However, these works have so far been validated only in simulation and phantom studies, and performance is sensitive to device position and orientation.

3 *WeeCare*

Our system design involves three phases:

- (1) **In-silico.** We perform a simulation-based design exploration to assess how electrode layout, noise, and non-ideal positioning affect system performance, which informs hardware design.
- (2) **In-vitro.** We conduct benchtop phantom validation to assess the effects of repeated pad removal and replacement, as well as urine salinity, which can vary with hydration and fluid intake.
- (3) **In-vivo.** We evaluate our bladder fullness sensing system on a human participant to characterize its feasibility under realistic physiological and repeated-placement conditions.

3.1 Simulation-based design exploration

3.1.1 Simulation setup.

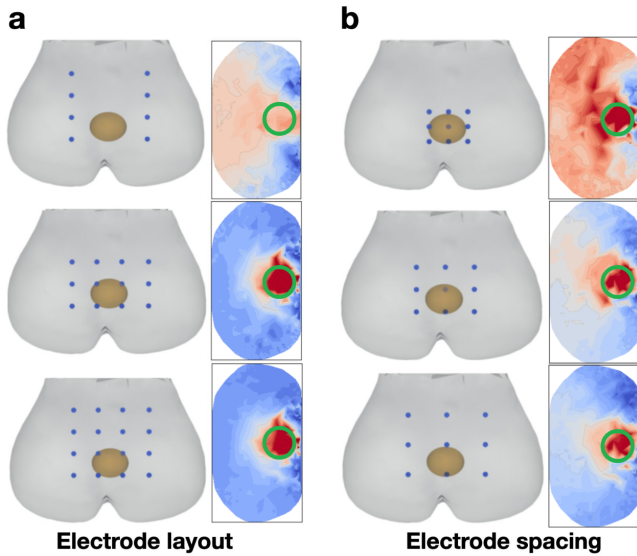


Figure 3: Simulation illustrating the effect of (a) electrode layout and (b) electrode spacing on EIT image reconstruction for a bladder filled to 100 mL. The figures show a 3D rendering of the abdomen and filled bladder, the electrode positions, and the 2D conductivity image reconstruction, slicing at the middle of the bladder. The green circle indicates the location of the bladder.

Table 1: RoI response ratios across electrode designs.

Variable	Configuration	RoI response ratio (R_{RoI})
Electrode count	2 × 4	1.91
	3 × 3	3.83
	3 × 4	8.15
	4 × 4	8.46
Electrode spacing (3 × 3)	30 mm	1.81
	45 mm	2.88
	60 mm	3.83

Torso and bladder model. To guide the design of our hardware system, we performed a simulation of our proposed planar electrode grid layout in PyEIT [25] to investigate how different electrode layout designs affect the reconstructed EIT image. For geometric simplicity, we simulate the abdomen using a custom torso mesh with 18,362 elements [16], and the bladder using an ellipsoid which captures how the bladder expands. Specifically, it captures how the bladder stretches at different rates along each axis, which an ellipsoid with three independent radii is able to capture [28].

Electrode channel selection. An EIT system produces readings for a large number of voltage channels, but much of that information is redundant as a change in bladder conductivity due to urine volume alters the entire electrical field at the abdomen and shows up across all electrodes. Using all these correlated channels for image reconstruction incurs unnecessary computational cost, so we sought to perform electrode down-selection to a smaller subset.

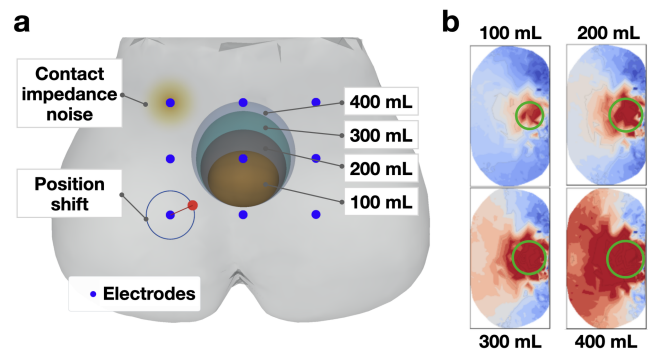


Figure 4: Effect of bladder volume under simulated electrode noise and movement. (a) Simulated bladder at different volumes and electrode perturbations. (b) Reconstructed conductivity images at different volume levels. The green circle indicates the area of the bladder.

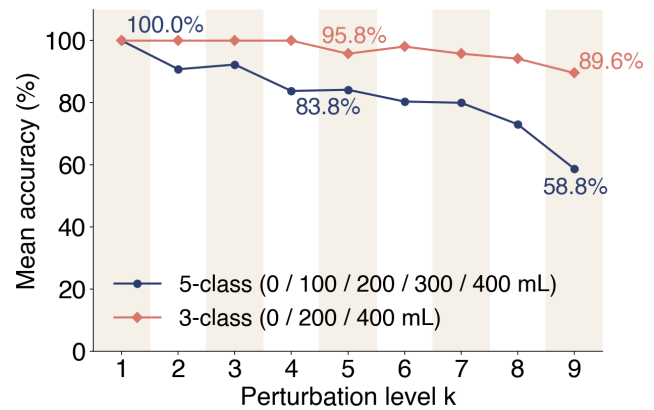


Figure 5: Effect of simulated electrode perturbation on bladder volume classification accuracy for different volume class divisions.

Using a concrete example of a 3 × 3 grid of $N = 9$ electrodes and 4-pole sensing, each channel uses four electrodes: one pair for current injection and one for voltage measurement (Fig. 2). The number of distinct channels is $\binom{9}{4} \cdot \binom{4}{2} = 756$, where $\binom{9}{4}$ counts the ways to choose four electrodes from nine and $\binom{4}{2}$ counts the ways to split those four into an injection pair and a sensing pair.

As acquiring all channels creates redundant information and increases measurement time, we perform channel down-selection. We retain two families of channels. The first uses 9 axis-aligned rectangles in the grid (every pair of rows with every pair of columns). For each rectangle we form channels by injecting current across one edge and measuring voltage across the opposite edge, yielding 36 channels. The second is a set of 12 diagonal channels, in which current injection and voltage sensing pairs are placed along the diagonals. Together these reduces the set to 48 channels.

Image reconstruction. The raw channel measurements are 1-D time-domain voltage signals, but bladder volume is inherently a spatial quantity. We reconstruct a 3D conductivity volume to better visualize changes in bladder volume.

For each channel, we first take the mean over a two-second window to suppress noise and produce one stable value per channel. We then perform baseline removal by treating the first frame of a session as a baseline and subtract it from all subsequent frames.

We then reconstruct a 3D volume of the relative change in abdomen area using the Jacobian-based reconstruction algorithm provided in PyEIT, with the regularization parameter set to $p = 0.5$, to control spatial smoothing. We then take a 2D image slice at the height of bladder center.

3.1.2 Effect of electrode layout. The electrode layout is an important design choice that dictates the physical size of the pad, as well as the number of contact points that must be reliably maintained against the skin. We therefore characterized two parameters that affect system performance: the number and configuration of electrodes, and the spacing between them.

For each electrode design, we simulated a bladder volume of 100 mL, reconstructed the corresponding 3D conductivity map, and quantified how well the reconstructed signal was localized to the bladder. Specifically, we computed the *RoI response ratio*, R_{RoI} , defined as the mean absolute reconstructed response inside the bladder region divided by that over the entire domain. Higher values indicate that the reconstructed response is, on average, stronger within the target bladder region than in the overall background.

Our results in Fig. 3 and Table 1 show that we first compared four electrode layouts: 2×4 , 3×4 , 4×4 and 3×3 . They show that more electrodes consistently produced higher RoI response ratios ranging from 1.91 for the smallest layout to 8.46 for the largest. We then varied electrode spacing across 30 mm, 45 mm, and 60 mm, and found that wider spacing also improved RoI response ratio.

Notably, though EIT is able to sense the conductivity change even with a small grid, a larger area of coverage provides improved spatial resolution across the entire region of interest. As a result, for our final hardware design, we select a large 3×3 grid as a practical compromise to emphasize portability and makes it easier to ensure reliable contact across all electrodes.

3.1.3 Effect of electrode perturbations. In the real-world electrodes may make uneven skin contact and differ slightly in placement between sessions. We therefore evaluate how well the system can distinguish between different urine volume levels under electrode noise and placement error (Fig. 4).

To set the number of volume classes, we treat 400 mL as the upper bound of our sensing range, since this is typically the level at which the urge to void becomes strong [44]. We divide this range into evenly spaced bins, yielding a 3-class problem (0, 200, 400 mL) and a 5-class problem (0, 100, 200, 300, 400 mL).

We apply two kinds of perturbation. The first is an impedance shift, where we scale the surface impedance near electrodes to 2–5x the nominal tissue impedance. The second is electrode relocation, where we displace electrodes from their intended positions to model placement error, ranging from 5 mm to 20 mm on the body. *These perturbation levels are intentionally large and are meant to stress-test the system beyond what would typically occur in practice.*

We parameterize the perturbation by its degree k where $k = 0$ means no perturbation, and $k = n$ means we randomly select n electrodes and apply random impedance shifts and relocations to

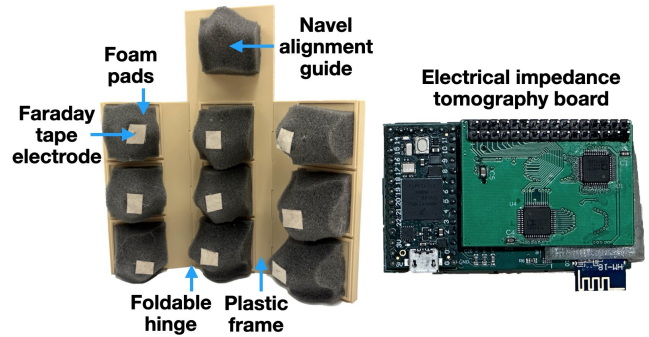


Figure 6: Handheld and conformable hardware prototype for bladder fullness sensing using EIT.

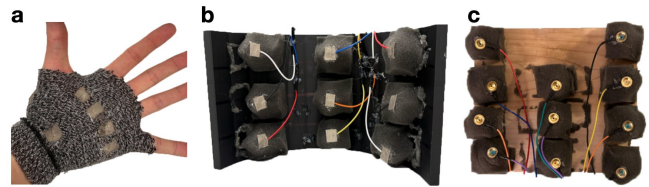


Figure 7: Alternative prototypes explored. (a) Glove form factor (b) Rigid curved frame (c) Gold-plated electrodes

them. Using a 3×3 grid, we sweep k from 1 to 9 and, at each volume level, perform 16 measurements under independent perturbations.

We then perform volume classification for the 3-class and 5-class problems. We train on all other perturbation levels and test on each one. We use the data from the 48 channels as input to the PyCaret library [1], which selected Logistic Regression as the best model. Our results in Fig. 5 show that with no perturbation ($k = 0$), we achieve 100% accuracy for both class divisions. For the 3-class division, this perfect accuracy holds until $k = 5$ where it decreases to 95.8%, and reaches 89.6% at $k = 9$. For the 5-class division, the decline is steeper, falling to 83.8% at $k = 5$ and 58.8% at $k = 9$.

3.2 Benchtop validation

3.2.1 Hardware design.

Sensor board. Our system (Fig. 6) builds on EIT-kit [50], which acquires bioimpedance measurements from multiple electrodes in a four-terminal measurement configuration. We use an excitation signal at a frequency of 50 kHz and a sampling rate of 3 Hz which is typically used for bladder sensing [23, 38].

Sensing pad. We use fabric Faraday tape electrodes [46] mounted on compressible foam pads [45], which provide more flexible placement than rigid electrodes, arranged in a 3×3 grid. To adapt to different abdomen geometries, the foam pads are attached to a foldable 3D-printed plastic frame with hinged joints that allows the system to conform to curved surfaces. For consistent placement, an extra foam pad above the grid is aligned to the navel, which provides a fixed anatomical reference across repeated measurements.

3.2.2 Prior design iterations. During the hardware design process, we also explored other form factors as shown in Fig. 7, but chose not to go forward with them for different reasons. *Form factor:* we investigated the use of a glove form factor, but found it was harder

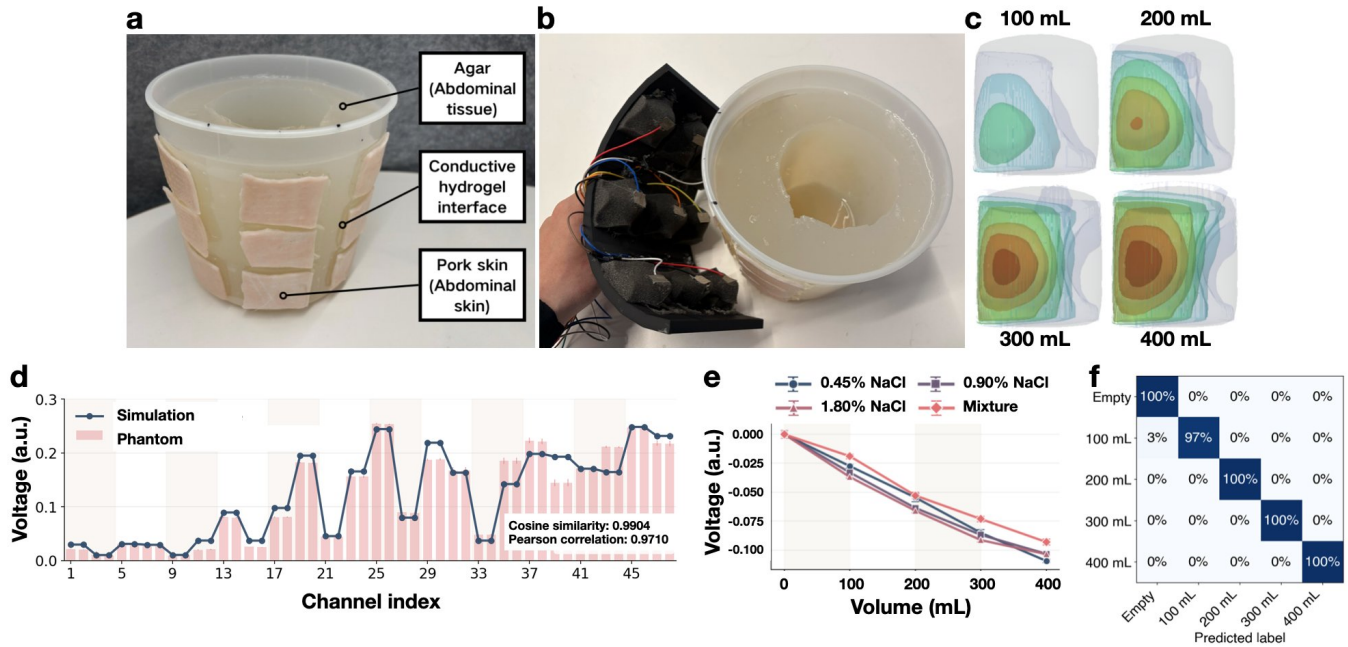


Figure 8: Benchtop validation on bladder phantom. (a) Abdomen simulating tissue, bladder, and skin. (b) WeeCare pad performing benchtop measurements on the phantom. (c) Reconstructed conductivity images from 100 to 400 mL. (d) Phantom voltage measurements show strong correlation with virtual simulation results. (e) Mean voltage decreases with bladder volume with similar trends across different urine salinities. (f) Confusion matrix for volume classification across different urine salinities.

to maintain consistent and stable contact across electrodes. *Frame*: we investigated a rigid plastic frame with a fixed curvature, but it did not adapt well to different abdomens shapes which negatively affected electrode contact and signal quality. *Electrodes*: we investigated the use of gold-plated electrodes, but found they did not provide better contact performance than the fabric electrodes. We opted for the fabric electrodes, as they are more conformable and comfortable against the skin, without the cold feel of metal.

3.2.3 Phantom design. We create a benchtop phantom to evaluate our system (Fig. 8a,b). To simulate abdominal tissue, we prepared a bowl of agar by boiling 2 L of tap water in a water distiller [5] and mixed in 16 g of agar powder [48] and 2 g of NaCl, which has a permittivity of $0.2S \cdot m^{-1}$, similar as soft tissue [34]. Once set, we hollowed out a 500 mL cavity at the center to represent the bladder. At each electrode position, we cut an opening in the bowl wall and applied a conductive hydrogel film [13] as a coupling interface, then layered pork skin over it to emulate abdominal skin.

3.2.4 Phantom validation results. We validated the phantom by comparing its channel-wise voltage responses to our simulation using a cylinder mesh to match the phantom (Fig. 8c). To do this we removed and replaced the pad from the phantom 8 times, normalized the amplitude, and plotted the average and standard deviation. We find that the cosine similarity across channels is 0.990 while the Pearson’s correlation is 0.971, showing a high level of similarity.

Finally, we investigate the effect of urine salinity on system performance given its effect on impedance [36]. We use 0.45%, 0.9%, and 1.8% NaCl water to simulate different salinities, which is

in line with known values [6, 33]. We take measurements across different volumes from 0 to 400 mL for uniform salinities, and for mixed salinities (a uniform mix of each salinity level). We take 8 measurement at each volume and salinity. We calibrated data of each salinity against a 0 mL baseline to eliminate baseline drift, as saline from previous tests may permeate into the agar.

All measurements are conducted at room temperature. We note that body-temperature urine ($\sim 37^\circ C$) would exhibit a higher baseline impedance than these measurements, however this can be compensated for using known relationships (approximately 2% per $^\circ C$). This compensation would not affect the volume classification task, which relies on relative rather than absolute changes.

As shown in Fig. 8e,f, the average voltage amplitude across channels decreases with volume for all tested salinity conditions. We then perform volume classification using leave-one-salinity-out using extra tree, on the 48 channels of data, and obtain a classification accuracy of 0.994 ± 0.013 . This shows that our system is robust to realistic variation in urine salinity concentration.

3.3 In-vivo evaluation

3.3.1 Data collection protocol. We evaluated our WeeCare system on one male participant aged 21, using a commercial ultrasound bladder scanner [42] (Fig. 9a) and ultrasound gel [32] as reference.

We collected three sessions of data, one per experiment day. Before each session, the participant avoided eating for two hours and arrived with a full bladder. We first measured the participant’s bladder as they voided and emptied their bladder, recording the global conductivity change on our device as a *voiding curve*. The

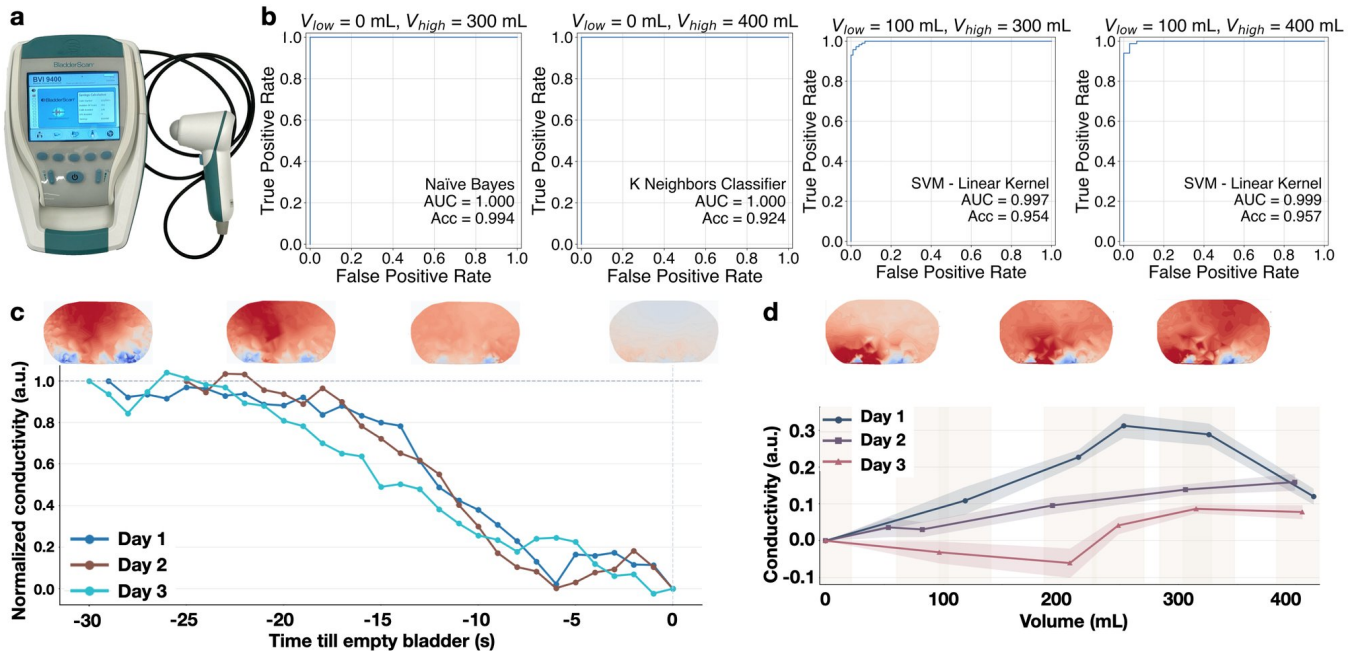


Figure 9: In-vivo evaluation. (a) Bladder ultrasound [42] used for ground truth measurement of bladder volume (b) Receiver operating curve for bladder fullness detection at different emptiness and fullness thresholds. (c) Voiding curve on three different days. (d) Filling curve on three different days, each captured over the course of several hours.

participant then gradually refilled their bladder by drinking water, with bladder volume monitored by the commercial ultrasound scanner every 10 minutes. At each checkpoint, we performed 8 repeated scans, discarded the maximum and minimum readings, and computed the mean of the remaining values. Once the measured volume approached the 200 mL and 400 mL states, or 20 minutes had elapsed since the last measurement, we performed 12 repeated measurements with our *WeeCare* system. For each measurement, we aligned the device to the navel landmark and lifted and replaced it on the abdomen. A small amount of conductive gel was applied to the electrodes to improve contact. After the final full-bladder measurement, the participant voided, and a final measurement of the empty bladder was taken. Between measurements, the participant moved freely; all measurements were taken while standing.

3.3.2 Results.

Bladder fullness detection. Using the EIT measurements from the filling protocol, we evaluated whether the system can distinguish between empty and full bladder states. We framed this as a binary classification task, labeling each measurement as positive when the bladder volume met or exceeded V_{high} and negative when it was at or below V_{low} . We assessed four (V_{low}, V_{high}) pairs (Fig. 9b): (0, 300), (0, 400), (100, 300), and (100, 400) mL. For each pair, we used PyCaret to compare candidate models and pick the one. Performance was evaluated under a leave-one-day-out scheme, using raw 48 channels data calibrated by the first empty frame within the day. Across all splits, the system separates the empty and full states with an AUC ranging from 0.997 to 1.000. Using a hard-decision threshold, binary accuracies ranged from 0.924 to 0.994.

Voiding dynamics. We show in Fig. 9c the change in conductance during voiding sessions on three separate days, each beginning when the bladder reached 400 mL, along with reconstructed 2D conductivity maps, at the estimated bladder area, for Day 2 showing the bladder region getting less conductive as voiding proceeds. We segmented each session into groups of three consecutive frames and averaged within each group to suppress noise. The resulting curves are amplitude-normalized to their starting point to illustrate the decrease observed over time. To assess day-to-day consistency, we computed the Pearson correlation between each pair of normalized curves, yielding an averaged $R = 0.80$. Each curve shows a similar decline over roughly 30 s, indicating that the system tracks voiding despite electrode removal and replacement between sessions.

Filling dynamics. We show in Fig. 9d the conductivity changes during the filling protocol across three days along with reconstructed 2D conductivity maps for Day 1. We observe that there is a general upward trend, however it is not completely monotonic. During a voiding event, which occurs in seconds, the impedance change can be attributed predominantly to the bladder, yielding a relatively clean monotonic decrease in conductivity. However, filling can occur over the span of hours during which muscle tension, intestinal motion, gas, and posture all shift the measured impedance [7, 22, 39]. As the bladder's contribution is entangled with these competing effects, the filling curve is not completely monotonic. For these reasons, we scope *WeeCare* to bladder fullness sensing rather than absolute volume estimation, which still answers the clinically relevant question of when catheterization is needed.

4 Limitations and discussion

Evaluation on diverse subjects. We present a proof-of-concept design of a handheld pad for bladder fullness sensing evaluated in-silico, in-vitro, and in-vivo. Further evaluation should include a broader population, particularly older adults and women. Urinary incontinence is common in older adults and is often linked to bladder dysfunction. Sex differences are relevant for bladder volume sensing and ultrasound scanners include separate modes for male and female patients to account for anatomical differences, such as the presence of the uterus, which displaces the bladder.

Device sanitization and gel. Like ultrasound imaging, our system requires a small amount of conductive gel at the electrode interface to displace air gaps and ensure consistent electrical contact with the skin. The device should also be wiped down between participants for hygiene. Unlike a rigid ultrasound probe, which must press firmly against the abdomen and can be uncomfortable, our pad is soft and conforms to the body.

References

- [1] Moez Ali. 2020. *PyCaret: An open source, low-code machine learning library in Python*. <https://www.pycaret.org>. PyCaret version 1.0.0.
- [2] Lynn Stothers Andrew J. Macnab. 2008. Near-infrared spectroscopy: validation of bladder-outlet obstruction assessment using non-invasive parameters. *Canadian Journal of Urology* 15, 5 (2008), 4241–4248. <http://www.techscience.com/CJU/v15n5/62252>
- [3] Benoit Brazey, Yassine Haddab, and Nabil Zemiti. 2022. Robust imaging using electrical impedance tomography: review of current tools. *Proceedings. Mathematical, Physical, and Engineering Sciences* 478 (2022). <https://api.semanticscholar.org/CorpusID:246445033>
- [4] Long Long Cao, Feng Wen Wang, Jingwei Xue, Fulei Liu, and Ming Liang Jin. 2026. Integrated Ultrasound Device for Precision Bladder Volume Monitoring via Acoustic Focusing and Machine Learning. *Advanced Science* 13, 17 (2026), e20926. [arXiv:https://advanced.onlinelibrary.wiley.com/doi/pdf/10.1002/adv.202520926](https://advanced.onlinelibrary.wiley.com/doi/pdf/10.1002/adv.202520926) doi:10.1002/adv.202520926
- [5] CO-Z. 2026. CO-Z 1.1 Gallon Water Distiller. <https://www.amazon.com/dp/B0D87F64BX> Accessed 2026-05-23.
- [6] Peter Curran and Simavita Limited. 2017. Everyday Monitoring of Incontinence Products: A New Disruptive Technology. Technical presentation. <https://announcements.asx.com.au/asxpdf/201711109/pdf/43p2lkbjrpntv.pdf> Presented at Hygienix 2017.
- [7] Kanika Dheman, Stefan Walser, Philipp Mayer, Manuel Eggimann, Marko Kozomara, Denise Franke, Thomas Hermanns, Hugo Sax, Simone Schürle, and Michele Magno. 2024. Noninvasive Urinary Bladder Volume Estimation With Artifact-Suppressed Bioimpedance Measurements. *IEEE Sensors Journal* 24, 2 (2024), 1633–1643. doi:10.1109/JSEN.2023.3324819
- [8] Peter T Dorsher and Peter M McIntosh. 2012. Neurogenic bladder. *Advances in urology* 2012, 1 (2012), 816274.
- [9] Lin Duan and Ming-Liang Jin. 2025. A biocompatible integrated bladder electronics for wireless capacity monitoring assessment. *Soft Science* 5, 1 (2025). doi:10.20517/ss.2024.46
- [10] Eoghan Dunne, Adam Santorelli, Brian Mc Ginley, Geraldine Leader, Martin O'Halloran, and Emily Porter. 2018. Image-based classification of bladder state using electrical impedance tomography. *Physiological Measurement* 39 (12 2018). doi:10.1088/1361-6579/aae6ed
- [11] Pascal Fechner, Fabian König, Wolfgang Kratsch, Jannik Lockl, and Maximilian Röglinger. 2023. Near-infrared spectroscopy for bladder monitoring: a machine learning approach. *ACM Transactions on Management Information Systems* 14, 2 (2023), 1–23.
- [12] Daniel D Fong, Xiaofan Yu, Jiageng Mao, Mahya Saffarpour, Prashant Gupta, Rami Abushsheikh, Alejandro Velazquez Alcantar, Eric A Kurzrock, and Soheil Ghiasi. 2018. Restoring the sense of bladder fullness for spinal cord injury patients. *Smart Health* 9 (2018), 12–22.
- [13] Generic Bio-Tech. 2026. Gel Pads for Abs Stimulator. <https://www.amazon.com/dp/B0FLJHG4C8> Accessed 2026-05-23.
- [14] David S. Holder (Ed.). 2005. *Electrical Impedance Tomography: Methods, History and Applications*. CRC Press.
- [15] Yasuhiko Igawa, Jean-Jacques Wyndaele, and Osamu Nishizawa. 2008. Catheterization: possible complications and their prevention and treatment. *International journal of urology* 15, 6 (2008), 481–485.
- [16] Kiwibunn. 2021. Female Torso Anatomy Study Sketch. <https://sketchfab.com/3d-models/female-torso-anatomy-study-sketch-5f186790eb5d436cad3b73b6117464d8>. Accessed: 2026-05-18.
- [17] F Krewer, F Morgan, E Jones, M Glavin, and M O'Halloran. 2014. Development of a wearable microwave bladder monitor for the management and treatment of urinary incontinence. In *Radar Sensor Technology XVIII*, Vol. 9077. SPIE, 295–303.
- [18] Niels Kristian Kristiansen, Hans Nygaard, and Jens Christian Djurhuus. 2005. Clinical evaluation of a novel ultrasound-based bladder volume monitor. *Scandinavian Journal of Urology and Nephrology* 39, 4 (2005), 321–328. [arXiv:https://doi.org/10.1080/00365590510031165](https://doi.org/10.1080/00365590510031165) doi:10.1080/00365590510031165 PMID: 16118108.
- [19] Eliza Lamin and Diane K Newman. 2016. Clean intermittent catheterization revisited. *International urology and nephrology* 48, 6 (2016), 931–939.
- [20] Kyungsu Lee, Moon Hwan Lee, Dongho Kang, Sewoong Kim, Jin Ho Chang, Seung-June Oh, and Jae Youn Hwang. 2024. Intelligent bladder volume monitoring for Wearable Ultrasound devices: enhancing Accuracy through Deep Learning-based coarse-to-fine shape estimation. *IEEE Transactions on Ultrasonics, Ferroelectrics, and Frequency Control* 71, 7 (2024), 775–785.
- [21] Steffen Leonhardt, Axel Cordes, Harry Plewa, Robert Pikkemaat, Irina Soljanik, Klaus Moehring, Hans J Gerner, and Rüdiger Rupp. 2011. Electric impedance tomography for monitoring volume and size of the urinary bladder. *Biomedizinische Technik. Biomedical engineering* 56, 6 (December 2011), 301–307. doi:10.1515/bmt.2011.022
- [22] Dorothea Leonhäuser, Carlos Castelar, Thomas Schlebusch, Martin Rohm, Rüdiger Rupp, Steffen Leonhardt, Marian Walter, and Joachim O. Grosse. 2018. Evaluation of electrical impedance tomography for determination of urinary bladder volume: comparison with standard ultrasound methods in healthy volunteers. *BioMedical Engineering OnLine* 17 (2018). <https://api.semanticscholar.org/CorpusID:51623929>
- [23] Rihui Li, Jinwu Gao, Yaning Li, Junpeng Wu, Zhanqi Zhao, and Yang Liu. 2016. Preliminary study of assessing bladder urinary volume using electrical impedance tomography. *Journal of Medical and Biological Engineering* 36, 1 (2016), 71–79.
- [24] Xuyang Li, Elena Pancera, Lukasz Niestoruk, Wilhelm Stork, and Thomas Zwick. 2010. Performance of an ultra wideband radar for detection of water accumulation in the human bladder. In *The 7th European Radar Conference*. IEEE, 212–215.
- [25] Benyuan Liu, Bin Yang, Canhua Xu, Junying Xia, Meng Dai, Zhenyu Ji, Fusheng You, Xiuzhen Dong, Xuetao Shi, and Feng Fu. 2018. pyEIT: A python based framework for Electrical Impedance Tomography. *SoftwareX* 7 (2018), 304–308.
- [26] H Madersbacher. 1990. The various types of neurogenic bladder dysfunction: an update of current therapeutic concepts. *Spinal Cord* 28, 4 (1990), 217–229.
- [27] Behnam Molavi, Babak Shadgan, Andrew J Macnab, and Guy A Dumont. 2013. Noninvasive optical monitoring of bladder filling to capacity using a wireless near infrared spectroscopy device. *IEEE transactions on biomedical circuits and systems* 8, 3 (2013), 325–333.
- [28] Anna S. Nagle, Adam P. Klausner, Jary Varghese, Rachel J. Bernardo, Andrew F. Colhoun, Robert W. Barbee, Laura R. Carucci, and John E. Speich. 2017. Quantification of bladder wall biomechanics during urodynamics: A methodologic investigation using ultrasound. *Journal of Biomechanics* 61 (2017), 232–241. doi:10.1016/j.jbiomech.2017.07.028
- [29] Shuhei S Noyori, Gojiro Nakagami, and Hiroimi Sanada. 2022. Non-invasive urine volume estimation in the bladder by electrical impedance-based methods: A review. *Medical Engineering & Physics* 101, 1 (2022), 103748.
- [30] Shuhei S Noyori, Gojiro Nakagami, and Hiroimi Sanada. 2022. Non-invasive urine volume estimation in the bladder by electrical impedance-based methods: A review. *Medical Engineering & Physics* 101 (2022), 103748. doi:10.1016/j.medengphy.2021.103748
- [31] M O'Halloran, F Morgan, M Glavin, E Jones, RC Conceio, and D Byrne. 2013. Bladder-state monitoring using ultra wideband radar. In *2013 7th European Conference on Antennas and Propagation (EuCAP)*. IEEE, 624–627.
- [32] Parker Laboratories Inc. [n.d.]. Aquasonic Ultrasound Gel Blue 1 Liter Bottle. https://www.amazon.com/dp/B07CX17646?ref_=ppx_hzsearch_conn_dt_bfed_asin_title_5. Accessed: 2026-05-05.
- [33] Nolan Perry. 2026. EIT for Bladder Monitoring: Principles, Methods, and Clinical Validation in Urodynamic Research. Biomedical Engineering Science. <https://www.biomedengsci.com/posts/eit-for-bladder-monitoring-principles-methods-and-clinical-validation-in-urodynamic-research> Accessed: 2026-05-25.
- [34] Aiyada Phisaiaphan, Phanpasorn Laor-Iam, Chamaiporn Sukjamsri, Anurak Dowloy, and Tawechai Ouypornkochagorn. 2025. Bladder monitoring with time-frequency-difference electrical impedance tomography technique. *Measurement* 250 (2025), 117162. doi:10.1016/j.measurement.2025.117162
- [35] Cong Pu, Ben Fu, Lehong Guo, Huixiong Xu, and Chang Peng. 2024. A Stretchable and Wearable Ultrasonic Transducer Array for Bladder Volume Monitoring Application. *IEEE Sensors Journal* 24, 10 (2024), 15875–15883. doi:10.1109/JSEN.2024.3382244
- [36] A E Rees, L C Ward, B H Cornish, and B J Thomas. 1999. Sensitivity of multiple frequency bioelectrical impedance analysis to changes in ion status. *Physiological Measurement* 20, 4 (nov 1999), 349. doi:10.1088/0967-3334/20/4/302

- [37] Gregory Samson and Diana D Cardenas. 2007. Neurogenic bladder in spinal cord injury. *Physical medicine and rehabilitation clinics of North America* 18, 2 (2007), 255–274.
- [38] Thomas Schlebusch, Steffen Nienke, S Leonhardt, and M Walter. 2014. Bladder volume estimation from electrical impedance tomography. *Physiological measurement* 35, 9 (2014), 1813–1823.
- [39] Seung-chul Shin, Junhyung Moon, Saewon Kye, Kyoungwoo Lee, Yong Seung Lee, and Hong-Goo Kang. 2017. Continuous bladder volume monitoring system for wearable applications. In *2017 39th Annual International Conference of the IEEE Engineering in Medicine and Biology Society (EMBC)*. 4435–4438. doi:10.1109/EMBC.2017.8037840
- [40] Alp Timucin Toymus, Umut Can Yener, Emine Bardakci, Özgür Deniz Temel, Ersin Koseoglu, Dincay Akcoren, Burak Eminoglu, Mohsin Ali, Rasim Kilic, Tufan Tarcan, et al. 2024. An integrated and flexible ultrasonic device for continuous bladder volume monitoring. *Nature Communications* 15, 1 (2024), 7216.
- [41] Verathon. 2018. BladderScan Prime Plus. <https://www.verathon.com/assets/0900-4510-xx-60.pdf>. Product brochure. Accessed: 2026-05-05.
- [42] Verathon Medical. 2008. BladderScan BVI 9400 Product Brochure. <https://www.verathon.com/sites/default/files/2021-08/0900-4412-xx-60.pdf>. Accessed: 2026-05-05.
- [43] Carla Verpoorten and Gunnar M Buyse. 2008. The neurogenic bladder: medical treatment. *Pediatric nephrology* 23, 5 (2008), 717–725.
- [44] Women’s Health and Education Center. 2009. Urodynamic Assessment: Techniques. <https://polylang.womenshealthsection.com/urog/urog003> Accessed: 2026-05-21.
- [45] WVOVW. 2026. 2”X12”X12” Sound Proofing Egg Crate Foam Pad. <https://www.amazon.com/dp/B0FP4K2CJB/> Accessed 2026-05-23.
- [46] WVOVW. 2026. Faraday Fabric Tape 1inch x 50 Feet Double Conductive High 1 Inch x 50. <https://www.amazon.com/dp/B097HPSLTH> Accessed 2026-05-23.
- [47] JJ Wyndaele. 2002. Complications of intermittent catheterization: their prevention and treatment. *Spinal cord* 40, 10 (2002), 536–541.
- [48] Yuantide Bio-Tech. 2026. Yuantide Bio Lab-Grade 100% Agar Agar Powder,150g / 5oz. <https://www.amazon.com/dp/B0CN41D2D4> Accessed 2026-05-23.
- [49] Ruoyu Zhang, Ruijie Fang, Chongzhou Fang, Houman Homayoun, and Gozde Goncu Berk. 2023. Privee: A wearable for real-time bladder monitoring system. In *Adjunct Proceedings of the 2023 ACM International Joint Conference on Pervasive and Ubiquitous Computing & the 2023 ACM International Symposium on Wearable Computing*. 291–295.
- [50] Junyi Zhu, Jackson C. Snowden, Joshua Verdejo, Emily Chen, Paul Zhang, Hamid Ghaednia, Joseph H. Schwab, and Stefanie Mueller. 2021. EIT-kit: An Electrical Impedance Tomography Toolkit for Health and Motion Sensing. In *Proceedings of the 34th Annual ACM Symposium on User Interface Software and Technology (UIST ’21)*. ACM, New York, NY, USA, 400–413. doi:10.1145/3472749.3474758